Computers, Materials & Continua

Tech Science Press

Doi:10.32604/cmc.2025.068878

ARTICLE

Improving Online Restore Performance of Backup Storage via Historical File Access Pattern

Ruidong Chen[1,#], **Guopeng Wang**[2,#], **Jingyuan Yang**[1], **Ziyu Wang**[1], **Fang Zou**[1], **Jia Sun**[1], **Xingpeng Tang**[1] **and Ting Chen**[1,*]

[1]School of Computer Science and Engineering (School of Cyber Security), University of Electronic Science and Technology of China, Chengdu, 611731, China

[2]Zhejiang Institute of Marine Economic Development, Zhejiang Ocean University, Zhoushan, 316022, China

*Corresponding Author: Ting Chen. Email: brokendragon@uestc.edu.cn

[#]These authors contributed equally to this work

Received: 09 June 2025; Accepted: 05 November 2025; Published: 12 January 2026

ABSTRACT: The performance of data restore is one of the key indicators of user experience for backup storage systems. Compared to the traditional offline restore process, online restore reduces downtime during backup restoration, allowing users to operate on already restored files while other files are still being restored. This approach improves availability during restoration tasks but suffers from a critical limitation: inconsistencies between the access sequence and the restore sequence. In many cases, the file a user needs to access at a given moment may not yet be restored, resulting in significant delays and poor user experience. To this end, we present Histore, which builds on the user's historical access sequence to schedule the restore sequence, in order to reduce users' access delayed time. Histore includes three restore approaches: (i) the frequency-based approach, which restores files based on historical file access frequencies and prioritizes ensuring the availability of frequently accessed files; (ii) the graph-based approach, which preferentially restores the frequently accessed files as well as their correlated files based on historical access patterns, and (iii) the trie-based approach, which restores particular files based on both users' real-time and historical access patterns to deduce and restore the files to be accessed in the near future. We implement a prototype of Histore and evaluate its performance from multiple perspectives. Trace-driven experiments on two datasets show that Histore significantly reduces users' delay time by 4-700× with only 1.0%–14.5% additional performance overhead.

KEYWORDS: Online restore; access pattern; correlation graph; trie

1 Introduction

Backups are widely used to increase the reliability of users' data against disasters [1–4]. However, it brings problems such as time-consuming restoration and increasing user delay time to access files. Take offline backup restore as an example, users need to wait until the entire backup is restored before they can access each file, usually taking several hours [5–8]. Online backup restore [9,10] allows users to recover backup in the background while performing operations such as reading and writing in the foreground. The user can operate on the restored files without waiting for the entire backup to be restored, thereby effectively reducing the user's delay time. To this end, we aim to further optimize online recovery performance, building on our preliminary work [11].

However, even with the online restore, there is a challenge in scheduling the restore sequence to match users' access sequence as closely as possible. Take a user's backup as an example. It contains file identifiers (denoted as fID_i) $\langle fID_1, fID_2, \ldots, fID_{10} \rangle$ and the restore sequence is $\langle fID_1, fID_2, \ldots, fID_{10} \rangle$. If the user's access sequence during restoration is $\langle fID_{10}, fID_9, fID_8, fID_7, fID_6 \rangle$, he will be delayed until the corresponding files are restored. This does not mitigate the long delay time. In contrast, if we adjust the restore sequence to $\langle fID_9, \ldots, fID_1, fID_{10} \rangle$, the user's delayed time can be significantly reduced.

This paper presents Histore, a backup storage system with improved users' experience in online restoration. The overall idea is to build on the user's historical access sequence to schedule the restore sequence, thereby reducing users' access delay time. Specifically, in the previous works, users' historical access information is widely used to predict the possible future user access to improve the availability of the file to be accessed [12–15]. The core design of Histore is three approaches that improve the online restore experience.

First, informed by the observation that the user's file access pattern is highly skewed [16], we propose a *frequency-based approach*, which prioritizes the restoration of the frequently accessed files. This ensures that most of the user's operations during the restoration process can be satisfied by already restored files. Also, inspired by the correlation of accessed files [14], we propose a *graph-based approach*, which establishes a correlation graph based on historical access patterns and generates the restore sequence (of files) via a greedy algorithm. Furthermore, we propose a *trie-based approach*, which combines users' historical and real-time access patterns to deduce (and restore) the files to be accessed in the near future.

To summarize, this paper makes the following contributions:

- We show via a case study that a baseline approach that restores files in alphabetical order incurs extremely high delay time, and hence significantly affects users' experience on foreground operations.
- We propose three restoration approaches to schedule the restore sequence of files based on historical access patterns.
- We design and implement Histore, a backup system that equips the three approaches to improve users' experience in online backup restore.
- We conduct extensive trace-driven experiments to evaluate Histore using two datasets. We show that all three proposed approaches can reduce users' delay by 4×–700× compared to the baseline, with 1.0%–14.5% performance overhead.

2 Background, Problem and Access Patterns

Background. We focus on backup workloads [17,18]. Specifically, we consider a *backup* as a complete copy of the primary data snapshotted from users' home directories or application states. Users periodically generate backups and store them in a storage system in order to protect their data against disasters, accidents, or malicious actions. Specifically, old backups can be restored either online or offline. That is, operate after complete restoration or operate while restoring. This paper focuses on *online backup restore*, which is widely deployed in existing cloud backup services [19]. It allows users to recover backups in the background while performing file operations in the foreground. Considering that backup restore often takes a long time [6], online restore significantly reduces the downtime since users can operate on the already restored files of the backup even if the whole backup is still under recovery.

One critical requirement for online restoration is to *minimize user-perceived performance degradation of the foreground operations*. Specifically, online restore recovers backups gradually in the background and needs to ensure that the operating files in the foreground have already been restored, in order to hide the performance degradation from the users.

However, to our knowledge, existing approaches (Section 6) focus on improving the overall restore speed, yet none of them are aware of minimizing user-perceived performance degradation. We establish a theoretical restore model (in contrast, we evaluate the practical online restore performance based on real-world access patterns in Section 5) to characterize the availability of users' foreground operations in the online restore procedure, and justify the problem based on the real-world file access trace collected by ourselves.

Theoretical restore model. We consider a set of unique files in a backup and define **A** as a sequence of the files (in the backup) that will be accessed in order by the foreground operations and **R** as a sequence of the files that will be restored in the background. Note that identical files may repeat in **A**, since users may apply the same operations multiple times or different operations may access the same files. On the other hand, each file in **R** appears only once, since the storage system does not need to restore identical files multiple times.

We consider a generic scenario in which the metadata of all unique files, as well as the contents of x% of the unique files in **R**, have already been restored offline. Then, users start the foreground access in **A**, while the restore process continues in the background. We focus on the availability level (see the measurements below) of **A** under different **R**, and make the following assumptions. First, the restoring of each file in **R** takes a constant time (called a *time slot*). Our rationale is that many frequently accessed files have small sizes (e.g., hundreds of KBs) [20], and the differences in their restore time can be negligible. For the large files (that are unlikely to be accessed in **A**), we can divide them into multiple small parts for restoration. Second, the duration that the foreground process stays on each file in **A** is equal to a time slot, such that the processing speeds of the files in **A** and **R** are synchronized. In fact, this captures the *worst availability* of online restore, since the foreground process may stay on a file for a long time (e.g., heavy edits), while the restore process is continuously running on different files. Finally, we do not consider resource contention, since we can limit the resource usage of the restore process.

We characterize two metrics to measure the performance of the foreground operations. The first metric is the *availability rate*, which is the number of successfully accessed files (i.e., these files have been restored when they are accessed) divided by the total number of accessed files. In addition, for the file that is unavailable for access, we consider its *delayed time*, which is the number of time slots when the file is available after it is accessed.

Simulation results. We study the availability of the foreground operations based on the real-world access log of a student (see Section 5 for dataset information). We focus on the access sequences of two consecutive days and consider a baseline approach that generates the restore sequence **R** based on the unique files of the first day *in alphabetical order*. Also, we use the access sequence of the second day to form **A**. Note that the files in **R** may not be in **A**, since the restored files may not be accessed immediately. Also, the files in **A** may not be in **R**, since the user may create and access new files (this implies that such files are available for access by nature). We evaluate the availability rate and delayed time of the baseline approach when the first 0%, 10%, and 30% of files in **R** have already been restored offline.

Fig. 1a presents the results for the availability rate (see theoretical restore model for metric definition), where the access ratio on the x-axis indicates the fraction of the files in **A** that are accessed. When $x = 0$ (i.e., no files have been restored before), the availability rate remains low (e.g., below 10%) for a significant fraction (e.g., about 14.0%) of access. This implies that the initial restored files in **R** cannot serve the corresponding file access in **A**. In contrast, if 10% of files have already been restored, the availability rate achieves up to 70.8% when 4.2% of files in **A** are accessed. This implies that restoring files in advance helps improve the availability of the accessed files. However, the availability rate then degrades, since the following restored files in **R** do not match the ones that are to be accessed in **A**. Fig. 1b shows the results for delayed time. We observe that the delayed time first dramatically increases with the access ratio, due to the mismatching of **R**

and **A**. Subsequently, the delay time tends to stabilize because only some files are accessed frequently, while most of these files have been restored and are available for access.

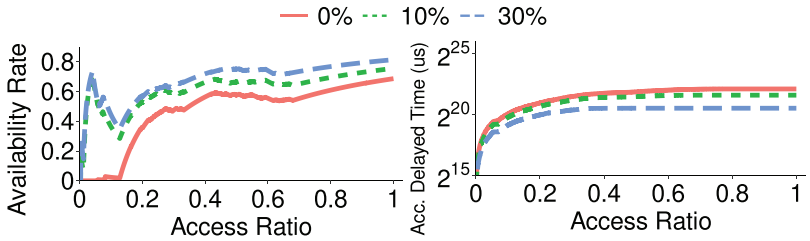

(a) Availability rate (b) Accumulated delayed time

Figure 1: Availability rate and accumulated delayed time with 0%, 10%, 30% files have been restored

In summary, we observe that the baseline approach incurs a low availability rate (especially for the initial file access in **A**) and extremely high delayed time, and hence significantly affects users' experience on foreground operations. This motivates us to improve online restore performance, especially ensuring that users' foreground operations can be served in time.

3 Restore Approaches

We build on previous file access prediction techniques [14,15], and propose three approaches to improve the online restore performance. Specifically, we assume that the sequence of historical access records $\mathbf{H}\langle fID_{r1}, fID_{r2}, \dots \rangle$ is known in advance. The frequency-based (Section 3.1) and graph-based (Section 3.2) approaches generate the restore sequence **R** of files all at once, while the trie-based approach (Section 3.3) gradually restores each target file (for restore) based on the user's real-time access patterns.

3.1 Frequency-Based Approach

Building on prior work [16], which shows that real-world file access distributions are skewed, we prioritize the restoration of frequently accessed files to ensure that the majority of operations in **A** are served promptly.

Algorithm 1 presents the details of the frequency-based approach. It takes the sequence of historical access records **H** as input and outputs the restore sequence **R** of files. It first initializes a map **M**, which maps each unique file ID to how many times (i.e., frequency) the file is accessed in **H** (Line 2). Specifically, it traverses each record in **H**, and increments the access frequency of a file if the file is indicated to be accessed in the record (Line 5). Otherwise, it inserts the (new) file ID into **M** and initializes the corresponding access frequency with one (Line 7). Finally, the algorithm sorts all file IDs by the corresponding access frequencies in descending order and returns **R** that includes the sorted file IDs (Line 11).

Algorithm 1: Frequency-based approach

```
1:  procedure FREQUENCY-RESTORE
    Input: sequence of historical access records H
    Output: restore sequence R
2:      Initialize a map M
3:      for each record r in H do
4:          if the file ID r.fID is in fMap then
```

(Continued)

Algorithm 1 (continued)

```
            M[r.fID] = M[r.fID] + 1
        else
            M[r.fID] = 1
        end if
    end for
    Sort M by access frequency
    return R = M
end procedure
```

3.2 Graph-Based Approach

The frequency-based approach does not capture the correlation of file access, while in practice, users may access a set of files together (rather than each file, individually). For example, when the user launches an application, the application program is likely to access a set of files in a deterministic order for initialization [21]. Previous work [14] builds on the access correlation among files to predict which file will be accessed in the future. Specifically, it partitions the sequence of historical file access records into many non-overlapped fixed-size windows, such that each window includes a number of file access records. It builds a directed graph to model file access patterns. Each node of the graph corresponds to a unique file, and stores how many times the file has been accessed, while each directed edge stores how many windows, in which the corresponding files are accessed in order. Given a currently accessed file, it predicates the file that is likely to be accessed as the one that connects with the current access file with the highest weight.

The insight of our graph-based approach is to prioritize the restoration of correlated files that are also frequently accessed in a short time. Specifically, we extend the above graph-based modeling by measuring access correlation based on a sliding window approach. Here, we configure a *sliding window* with a fixed size of five access records and count how likely a file is to be co-accessed with other files in the same sliding window. Also, we construct an undigraph such that each edge stores the number of times that the corresponding files are co-accessed in identical sliding windows. Based on the graph, we use a greedy algorithm to generate the restore sequence **R** of files. Specifically, each time, we choose the edge that has the largest weight and include the corresponding files into **R**, so as to first restore the frequently accessed correlated files.

Algorithm 2 presents the details of the graph construction algorithm, which takes the sequence of historical records as input. It first initializes an empty $\mathcal{G}$ (Line 2) and queue W (Line 3). For each record r in **H**, it adds r into W (Line 5). If W is full, it calls the UPDATE algorithm to update the graph based on the *co-access occurrences* of the file ID in front of W with each following file ID (Line 7). Our rationale is to avoid repeated counting when the window slides. Then, it removes the front file ID from W (Line 8). It finally returns the graph $\mathcal{G}$ until all records in **H** have been processed (Line 11).

Algorithm 2: Building graph

```
1:  procedure GRAPH-BUILDING
    Input: sequence of historical access records H
    Output: graph G = (V, E)
2:      Initialize G = (V, E) as an empty graph
3:      Initialize a sliding window queue W with the capacity λ
4:      for each record r in H do
```

(Continued)

Algorithm 2 (continued)

```
 5:            W. Enqueue(r.fID)
 6:            if |W| == λ then
 7:               G = Update (W, G)
 8:               W. Dequeue()
 9:            end if
10:      end for
11:      return G
12:   end procedure
13:   function Update
        Input: sliding window W, graph G = (V, E)
14:       fID_s = fID in the front of W
15:       G.V = G.V ∪ {fID_s}
16:       for each fID in W − {fID_s} do
17:             G.V = G.V ∪ {fID}
18:             if {fID_s, fID} ∈ G.E then
19:                   G.E[{fID_s, fID}] = G.E[{fID_s, fID}] + 1
20:             else
21:                G.E[{fID_s, fID}] = 1
22:             end if
23:       end for
24:   end function
```

The Update algorithm takes a sliding window W and the graph $\mathcal{G} = (V, \mathbf{E})$ as input, where V is the set of file IDs (as the vertices of $\mathcal{G}$) and $\mathbf{E}$ is an associate array that maps a pair of file IDs to the weight of the corresponding edge (of $\mathcal{G}$). It first includes the file ID fID_s in the front of W into the graph (Line 15). For any other file ID fID in W, if the edge $\{fID_s, fID\}$ has been stored in the graph, it increments the corresponding weight by one (Line 19). Otherwise, it creates a new edge for $\{fID_s, fID\}$ in the graph and initializes the corresponding weight with one (Line 21).

Algorithm 3 shows the greedy-based file restoration algorithm, which builds on the updated graph $\mathcal{G} = (V, \mathbf{E})$ to gradually generate the restore sequence $\mathbf{R}$. Specifically, it initializes $\mathbf{R}$ as an empty sequence (Line 2). In the main loop, it first chooses the edge $\{fID, fID'\}$ that has the largest weight in $\mathcal{G}.\mathbf{E}$ and appends fID and $fID\prime$ into $\mathbf{R}$ (Lines 4–5). It also removes them from $\mathcal{G}.V$ and $\mathcal{G}.\mathbf{E}$ (Lines 6–7). Then, it iteratively finds fID^* in $\mathcal{G}.V$ that connects to existing file IDs in $\mathbf{R}$ with the largest weight (among other file IDs in $\mathcal{G}.V$). Specifically, if no file ID is found (Line 10), it breaks the loop to find the largest weight edge (see above). Otherwise, it appends such fID^* into $\mathbf{R}$, and removes the fID^* and the corresponding edge from $\mathcal{G}.V$ and $\mathcal{G}.\mathbf{E}$, respectively (Lines 13–15). The algorithm finally returns $\mathbf{R}$ until all file IDs in $\mathcal{G}.V$ have been added into $\mathbf{R}$ (Line 18).

Algorithm 3: Generating restore sequence based on graph

```
 1: procedure Restore-gen
    Input: graph G
    Output: restore sequence R
 2:     Initialize R as an empty sequence
 3:     while G.V is not empty do
```

(Continued)

Algorithm 3 (continued)

```
        Choose {fID, fID'} that has the largest weight in G.E
        Append fID and fID' into R
        Remove {fID, fID'} from G.E
        G.V = G.V − {fID, fID'}
        while G.V is not empty do
            Find {fID, fID*} ∈ G.E that has the largest weight among all fID ∈ R and fID* ∈ G.V
            if {fID, fID*} does not exist in G.E then
                Break
            end if
            G.V = G.V − {fID*}
            Append fID* into R
            Remove {fID, fID*} from G.E
        end while
    end while
    return R
end procedure
```

3.3 Trie-Based Approach

Both frequency-based and graph-based approaches generate the restore sequence **R** all at once. However, in practice, users' access patterns are dynamic and subject to change. To adapt to dynamic changes in access patterns, we propose a trie-based approach to gradually generate **R** based on users' real-time access patterns, in addition to the sequence of the historical access files **H**.

The proposed trie-based approach extends the principles of *partitioned context modeling (PCM)* [15], which predicts the occurrence of a symbol using a trie structure. In PCM, each trie node represents a symbol and stores its occurrence count (referred to as weight) relative to its parent node. An edge in the trie connects two symbols that co-occur, with the parent node representing the first symbol and the child node representing the subsequent symbol. For a given input string (a sequence of symbols), PCM traces a path from the root to a non-leaf node and predicts the next symbol based on the most probable continuation along the path.

We adapt PCM to predict file access patterns based on real-time user behavior. Our trie-based method operates in two stages. In the first stage, the trie is constructed using the historical sequence **H** of accessed files. A *variable-sized* sliding window W is utilized to scan **H**. The window size increases incrementally if the sequence of file IDs in W matches an existing *path* in the trie (from the root to an internal node). If no match is found, the window size is expanded to identify and incorporate longer access patterns into the trie.

In the second stage, the constructed trie is used to predict the next file to be accessed. If the predicted file is not yet restored, it is pre-emptively restored. Otherwise, the file with the highest access frequency in **H** is selected for restoration.

In the prediction process, the trie uses a sequence of recently accessed file IDs, derived from users' real-time access patterns, to match a path in the trie. It selects the child node (i.e., the file ID) connected to the path with the largest weight. If no matching path exists, no subsequent node is found after the path, or the predicted file has already been restored, the sequence of recently accessed file IDs is updated to retain only the most recent items, reducing the sliding window size. The process then attempts prediction again. The rationale here corresponds to the case of decreasing the sliding window size after finding a new path in

the trie-building process. In essence, the approach ensures that a shorter matched path is considered. If the shorter path also fails, the process falls back to the basic case of using only the most recently accessed file ID for prediction.

Algorithm 4 presents the pseudocode of the trie construction algorithm. It takes the sequence **H** of historical records, as well as the minimum min (e.g., 3) and maximum max (e.g., 5) sizes of the sliding window as input. It starts by filling a minimum sliding window W with the first $min - 1$ records of **H** for initialization (Lines 2–4).

Algorithm 4: Building trie

```
1:  procedure TRIE-BUILDING
    Input: sequence of historical access records H, minimum sliding window size min, maximum
      sliding window size max
    Output: trie 𝒯
2:      Initialize a sliding window queue W with capacity min
3:      Initialize a trie 𝒯 with only a root node
4:      Move the first min − 1 records of H into W
5:      for each record r in H do
6:          W. ENQUEUE(r)
7:          if W does not correspond to a path in 𝒯 or |W| = max then
8:              UPDATE (W, 𝒯)
9:              Run W.DEQUEUE for |W| − min + 1 times
10:         end if
11:     end for
12:     if |W| ≥ min then
13:         UPDATE (W, 𝒯)
14:     end if
15:     return 𝒯
16: end procedure
17: function UPDATE
    Input: a queue W of file IDs, trie 𝒯
18:     Initialize node_cur = 𝒯 · root
19:     for each record r in W do
20:         if r.fID does not correspond to any child node of node_cur then
21:             Insert a new child node r.fID for node_cur
22:         end if
23:         node_cur = node_cur.child[r.fID]
24:         node_cur.weight = node_cur.weight + 1
25:     end for
26: end function
```

In the main loop, it adds the record r into W (Line 6). If the file IDs in W do not form a path of the trie or W achieves the maximum window size, the algorithm updates the trie based on existing records in W (Line 8) and then removes the first $|W| - min + 1$ records from W (Line 9). After all records in **H** have been processed, the algorithm updates $\mathcal{T}$ based on the remaining records of W (Lines 12-14), and returns $\mathcal{T}$ (Line 15).

The UPDATE algorithm takes the sliding window W and the trie $\mathcal{T}$ as input. It first initializes a pointer $node_{cur}$ that points to the root of the trie (Line 18). For each record r in W, if r does not correspond to any child node of $node_{cur}$, it initializes a new node for r and inserts the new node as a child of $node_{cur}$ (Lines 20–22). Also, it moves $node_{cur}$ to the child node corresponding to r and increments the weight (Lines 23–24).

Algorithm 5 presents the trie prediction algorithm to predict file access sequence. It takes the trie $\mathcal{T}$, the currently accessed file fID_x, the minimum min and maximum max sliding window sizes, and the list **L** of historically accessed files that are sorted by access frequencies as input. It initializes three data structures: (i) D, which stores the files that are delayed to be restored; (ii) W, which stores a sliding window of file IDs; and (iii) R, which stores the already restored files. If fID_x has not been restored, the algorithm inserts fID_x into **D** (Lines 5–7). Also, the algorithm enqueues fID_x into W (Line 8), and removes the first $max - min + 1$ IDs from W if W achieves the maximum size. Then, the algorithm attempts to predict the file to be accessed next based on the trie, W and R, and returns fID_y (Line 12).

Algorithm 5: Trie prediction algorithm

```
1:  procedure TRIE-PREDICTION
    Input: the trie T, current accessed file fID_x, minimum sliding window size min, maximum sliding
      window size max, list L of historical accessed files that are sorted by frequency
    Output: the file ID fID_y to be accesed next
2:      Initialize queue D to record files that are delayed to be restored
3:      Initialize set R to record already restored files
4:      Initialize sliding window W
5:      if fID_x is not in R then
6:          D.ENQUEUE(fID_x)
7:      end if
8:      W.ENQUEUE(x)
9:      if |W| = max then
10:         delete first max − min + 1 IDs from W
11:     end if
12:     fID_y = PREDICT(W, R, T)
13:     if fID_y = null then
14:         if |W| ≥ min then
15:             delete first |W| − min + 1 IDs from W
16:             fID_y = PREDICT(W, R, T)
17:         end if
18:         if fID_y = null then
19:             delete first |W| − 1 IDs from W
20:             fID_y = PREDICT(W, R, T)
21:             if fID_y = null then
22:                 if D is not empty then
23:                     fID_y = D.DEQUEUE()
24:                 else
25:                     select the most frequently accessed file from L as fID_y
26:                 end if
27:             end if
```

(Continued)

Algorithm 5 (continued)

```
28:              end if
29:            end if
30:            Include fID_y into R
31:            Remove fID_y from D
32:            Remove fID_y from L
33:            return fID_y
34:    end procedure
35:
36:    function PREDICT
         Input: queue W, R and trie T
         Output: predicted next access file fID_y
37:          Initialize node_cur = T.root and fID_y = null
38:          for each fID_r in W do
39:              if fID_r doesn't correspond to any child of node_cur then
40:                  node_cur = nullptr
41:                  break
42:              else
43:                  node_cur = node_cur.child[fID_r]
44:              end if
45:          end for
46:          if node_cur · child! = null then
47:              select node with largest weight in node_cur.child that doesn't appear in R
48:              fID_y = node.fID
49:          end if
50:          return fID_y
51:    end function
```

Note that fID_y may be *NULL* in simple prediction (see our example below). Then, the algorithm attempts to resize W in order to reduce the length of the necessary matching path of the trie. Specifically, it first removes the first $|W| - min + 1$ IDs from W if W's size is not less than min, and predicts fID_y (Lines 14–17). If the prediction result is still *NULL*, the algorithm reduces the size of W and re-predicts fID_y based on only a single ID in W (Lines 18–20). If the last attempt fails (i.e., the prediction result is still *NULL*) and D is not empty, it sets fID_y as the first file that is delayed to be restored in D (Lines 22–24). Otherwise, if D is empty, it chooses the unrestored file that is most frequently accessed in history as fID_y (Lines 25–26). Finally, it adds fID_y as the restored file, removes fID_y from **D**, removes fID_y from **L** and returns fID_y (Lines 30–33).

The PREDICT function takes the recent access file queue **W**, restored file queue **R**, and the trie $\mathcal{T}$ as input. It initializes a pointer to $\mathcal{T}$'s root and the file to return y (Line 37). For each record in **W** (Line 38), if $\mathcal{T}$ doesn't have a corresponding node (Line 39), move the pointer to nullptr and break (Line 40–41). Otherwise, then move the pointer and continue to judge (Line 43). If all items in **W** have a corresponding node in $\mathcal{T}$ (Line 46), it selects the unrestored node with the largest weight among the children of the **W**'s last item (Line 47–48).

Example. We present an example to illustrate the trie-based approach. Let the minimum and maximum window sizes be 3 and 5, respectively, and consider a historical sequence of accessed files **H** =

$\langle A, B, A, C, D, A, B, A, B, C, A, B, C, D, A, B, C, D, E, A\rangle$. The sequence is scanned to generate multiple variable-sized sliding windows of file IDs, which are then used to update the trie (Line 8 in Algorithm 4).

For instance, after scanning the first seven file IDs, sliding windows such as $\langle A, B, A\rangle$, $\langle B, A, C\rangle$, $\langle A, C, D\rangle$, $\langle C, D, A\rangle$, and $\langle D, A, B\rangle$ are identified and inserted into the trie. As the sliding window progresses, patterns matching existing trie paths are extended by increasing the window size. For example, $\langle A, B, A\rangle$ matches a trie path, so the window is extended to $\langle A, B, A, B\rangle$, which is then added to the trie. Similarly, other windows such as $\langle A, B, C\rangle$, $\langle B, C, A\rangle$, $\langle C, A, B\rangle$, $\langle A, B, C, D\rangle$, $\langle C, D, A, B\rangle$, $\langle A, B, C, D, E\rangle$, and $\langle D, E, A\rangle$ are processed, leading to the final trie structure shown in Fig. 2.

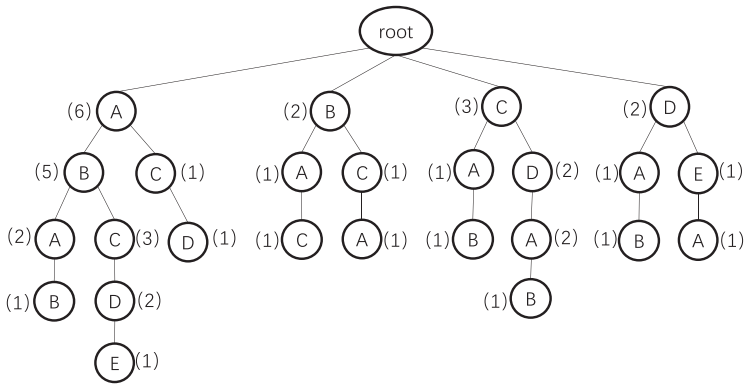

Figure 2: Example of constructing trie with minimum sliding window size of 3 and max size of 5 for the historical sequence ⟨ A, B, A, C, D, A, B, A, B, C, A, B, C, D, A, B, C, D, E, A ⟩

Next, assume the ground truth of the user's access sequence is $\langle C, D, A, B, B, E\rangle$. Using the trie, predictions for file restoration are made as follows. Starting with the first accessed file C, we predict D (the most likely file to follow C) and restore it before the user accesses it. Similarly, A (following D) and B (following A) are restored in advance. However, when the user accesses B again, no prediction is possible because the path $\langle C, D, A, B\rangle$ terminates (i.e., B has no child nodes). At this point, the first two IDs, C and D, are dequeued (Line 15 in Algorithm 5), and the next file predicted is C (the most likely file following $\langle A, B\rangle$).

When the user accesses B again, the sliding window $\mathbf{W} = \langle A, B, B\rangle$ does not match any path in the trie $\mathcal{T}$, resulting in a prediction failure (Line 12 in Algorithm 5). After handling the failure case (Lines 14–21), the algorithm checks whether the delayed restore queue D is empty (Line 22). Initially, C is enqueued into D when the user first accesses it, but on the fourth access (B), C is dequeued after being predicted. At this point, D becomes empty. The algorithm then selects an unrestored file with the highest frequency. Since only E remains unrestored, E is predicted (Line 25). After restoring E, all unique files are restored, ensuring that subsequent accesses succeed.

The final restore sequence generated by the prediction algorithm is $\langle D, A, B, C, E\rangle$.

4 Design and Implementation

We present Histore for outsourced backup management. Histore provides a *client*, which realizes an interface to outsource (restore) backups to (from) a remote *cloud* server. The client implements online restore approaches (Section 3) that can improve users' online restore experience based on historical access patterns. Specifically, to capture historical access patterns, we assume that the cloud maintains access logs about users. We argue that the assumption is practical since many service providers track users' access statistics to improve the quality of service [22–25]. Our current Histore prototype includes 5.3 K lines of code (LoC) of C++ code.

4.1 Store Management

To store a backup, a client first collects the file metadata (e.g., name and size), as well as the ownership information (e.g., the identifier of the user that processes the backup). and then transmit both file data and metadata to the cloud.

The cloud maintains two key-value stores (both of which are implemented via LevelDB [26]) to manage the metadata information. Specifically, the *file index* maps each backup's file pathnames to the corresponding files' metadata, such as size. The *user index* maps each user identifier to the latest backup version number of the user.

To manage stored backups, Histore maintains a home directory for each available client. When a client stores a backup, the cloud creates a version directory to store the backup's files. Here, in the version directory, we preserve the original filename of each file in a backup. In addition to backup contents, the cloud manages a log file `access.log` in the version directory to record the historical access pattern of the corresponding backup. In our current implementation of Histore, the cloud only keeps the most recent K backups. If the client stores the $K+1$-th backup, the cloud automatically removes the oldest backup.

4.2 Restore Management

Histore implements three restoration approaches (Section 3), allowing clients to select their preferred method. Specifically, upon receiving a restore request from a client, the cloud decides which files in the corresponding backup need to be restored first. The cloud generates a stored file list for the backup, where items are sorted by historical access frequency. The frequency-based approach directly restores each file based on the list.

In the graph-based approach, Histore implements the graph via an adjacency list shown as Fig. 3a, as well as stores the edge weights in a hash table shown as Fig. 3b. The hashtable is mainly used to speed up the process of graph building.

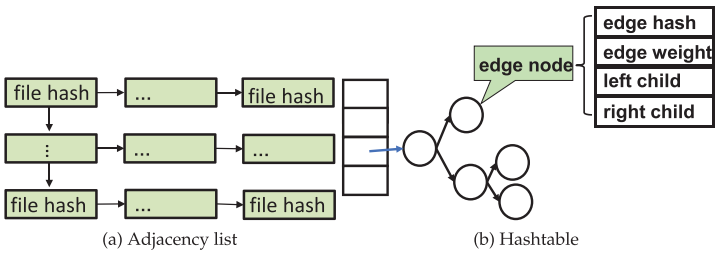

Figure 3: Key data structures used in the graph-based approach

The index of the hashtable is computed as the hash of an edge, derived from the hashes of the two file pathnames. The corresponding value in the hashtable is a *Binary Sort Tree* [27], which resolves hash collisions. This structure enables efficient edge lookup during insertion to determine whether the edge already exists. If the edge does not exist, a new node is appended to the binary tree; otherwise, the weight of the existing node is updated.

The adjacency list is employed to accelerate graph splitting. The head nodes of the adjacency list store all vertices of the graph (represented by the hashes of file pathnames), while the adjacent vertices of each node are stored as entries following the corresponding head node. During graph splitting, the greedy algorithm iteratively retrieves a vertex's adjacent vertices and removes edges from the graph. With the adjacency

list, locating a vertex's neighbors only requires traversing its head node, and edge deletion involves simply removing the corresponding entries.

In the trie-based approach, the trie is implemented as a *multi-fork tree*, where each node maintains the filename, its weight, and a *child map*. The child map stores mappings between filenames and pointers to their respective child nodes.

To restore a backup, the client sends a restore request to the cloud. The cloud first retrieves the user's latest backup version using the *user index*. If the frequency-based or graph-based method is selected, the cloud invokes the corresponding module to generate the restore sequence R using `access.log`, sending file pathnames, sizes, and content to the client in the order specified by R. If the trie-based method is used, the cloud initializes the trie structure from `access.log`. Concurrently, the client periodically transmits the most recent access sequence (five items at a time) to the cloud, which uses this sequence to predict subsequent restore targets. Once the entire backup is transmitted, the cloud signals completion by sending a flag to the client before closing the connection.

4.3 Optimization

We adapt the commonly used multi-threading optimization techniques to parallelize the communication, processing, and storage I/O of the cloud in the pipeline. Also, we are multi-threading the service for different clients.

4.4 Discussion

Histore currently focuses on scenarios where a single cloud server processes unencrypted plaintext backups. In this section, we address the potential limitations under such a scenario.

Distributed cloud storage. At present, Histore only supports backup restoration using a single cloud server. To enhance scalability and support distributed storage, Histore can partition backups and store them across multiple storage backends. During restoration, these backends can operate in parallel, significantly improving the throughput of Histore. However, this approach reduces system reliability, as the failure of any storage backend may render part or all of the backup unrecoverable, leading to restoration failure. To mitigate this issue, redundant storage [28] or erasure coding technique [29] can be employed to improve system stability and ensure data recovery in the presence of backend failures.

Data security. Currently, Histore handles plaintext backup content in the cloud. Given that the cloud and client often belong to different organizations and third-party cloud providers operate in potentially vulnerable network environments [30,31], users may distrust cloud memory and persistent storage devices [32]. To ensure data confidentiality, backups can be encrypted on a per-file basis at the client side prior to upload and decrypted during restoration. However, as the proposed methods (Section 3) rely on access patterns and metadata, these inevitably become exposed to the cloud, introducing the risk of side-channel attacks. While existing techniques, such as Oblivious RAM [33,34], can fully obscure access patterns and metadata, they conflict with the design goals of Histore. Addressing this limitation remains an open problem for future work.

5 Evaluation

5.1 Setup

Datasets. We use two mixed datasets to drive our evaluation. The first dataset is *mix-1*. We use the process monitor [35] to collect the file system, registry, and process/thread activities of a student's machine (that runs Windows 10) in our research group in the period of June 19 to June 25, 2021. We exclude the system

directories `Windows`, `ProgramData`, `Intel`, `AMD`, and `Drivers` (if the latter three exist), and focus on the `readFile` and `writeFile` operations that are applied on the remaining files. We merge multiple consecutive reads (writes) on an identical file into one read (write) to the file.

However, since our collected logs do not contain file metadata, we associate each unique file record in the access log with a file in the FSL snapshots, which represent daily backups of students' home directories from a shared network file system [36]. Each FSL snapshot consists of a sequence of file names and their corresponding sizes. We choose two FSL snapshots with as many files as access logs and write random values repeatedly to each file (in these snapshots) with the specified size. We then map each file record of the access log to a replayed file in the FSL snapshots based on the principle that small files are likely to be accessed frequently. The mix-1 dataset contains the file access data of the same user for 2 consecutive days, and the dataset finally includes 59 GiB of file data.

The second dataset is *mix-2*, which maps on access records in the Microsoft Research Cambridge (*MSRC*) dataset [37] to files in the *MS* dataset [38]. Specifically, the MSRC dataset includes the block-level access records collected from multiple servers, and we focus on the directory *hm_1*. Note that we assume that each independent access block corresponds to a distinct file. Since the MS dataset only contains a list of file metadata, which is similar to that in FSL, we randomly choose three MS snapshots and generate synthetic files with random content based on the metadata and map the files to the access sequence in *hm_1* based on the principle that small files are accessed more frequently. The resulting mix-2 dataset contains 333 GiB of file data.

Testbeds. We configure a LAN cluster for the cloud and multiple clients. We have two types of machines: host and cloud. Our host machines are equipped with an 8-core 2.9 GHz Intel Core i7-10700 CPU, 32 GB RAM, and a 512 GB Non-Volatile Memory Express (NVMe) SSD alongside a 4 TB 7200 rpm SATA HDD. While our cloud machine has a 16-core 2.1 GHz Intel Xeon E5-2683 v4 CPU, 64 GB RAM, and a RAID 5 disk array based on four 4 TB 7200 rpm SATA HDD. All machines are running Ubuntu 20.04 LTS and connected with a 10 Gigabit Switch.

5.2 Theoretical Analysis

To illustrate the effectiveness of the three restoration approaches, we followed the simulation (see Section 2 for details) to compare the availability ratio and delayed time of the three approaches to the baseline approach. We split the two datasets *mix-1* and *mix-2* to generate historical access sequences **H** and current access sequences **A**, and generate different restore sequences **R** based on **H** and **A**. Specificity, for the *mix-1* dataset, we use the user's access sequence of two consecutive days, taking the access sequence on the first day as the historical access sequence **H** and the access sequence on the second day as the user's current access sequence **A**. For the *mix-2* dataset, we equally divide the MSRC's access sequence into two equal parts. The first half is **H**, and the second half is **A**.

Here, we run the cloud program on our cloud machine and the client's program on the host machine, while setting the network bandwidth as 100 MiB/s to get each file's restored time. We evaluate the *availability rate*, which is the number of successfully accessed files divided by the total number of current accessed files. In addition, we consider *delayed time rate* as the current cumulative delayed time of the target approach divided by the baseline approach's cumulative delayed time.

Fig. 4a,b shows the theory availability ratio of four restoration approaches changes with the restoration process. For both *mix-1* and *mix-2* datasets, with the *Frequency*, *Graph* and *Trie* restore sequence, the system can achieve more than 99% availability ratio after restoring about 7% of the files, while with the baseline (*alphabetical*) restore sequence, it can only reach 50%–70% and 12% for the mix-1 and mix-2 datasets,

respectively. We noticed that the availability ratio of the baseline approach differs significantly in the two datasets. This is because the name of the frequently accessed file in **A** of the *mix-1* dataset is at the top of the alphabetical sequence.

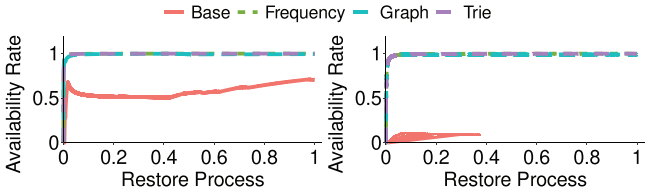

Figure 4: Availability ratio of two datasets on different restoration approaches. The *x*-axis presents the whole restore process

Fig. 5a,b shows the delayed time ratio of four restoration approaches when processing the two datasets. Since the cumulative delayed time of the baseline is the denominator for calculating the delayed time rate, its delayed time ratio is always kept as 1 (the red line), and the lower the delayed time rate, the lower the access delayed time than the baseline. For both *mix-1* and *mix-2* datasets, the three approaches can effectively reduce the delayed time in the whole process. For the *mix-1* dataset, the frequency-based approach is the best that could reduce the delayed time by up to 99.7%. While the graph-based approach is the worst, which could only reduce the delayed time by 94%. In addition, for the *mix-2* dataset, the graph approach first reduces the delayed time, then increases the delayed time by a part. This is mainly because the graph approach utilizes the principle of the local optimal solution used, which is not globally optimal on the *mix-2* dataset.

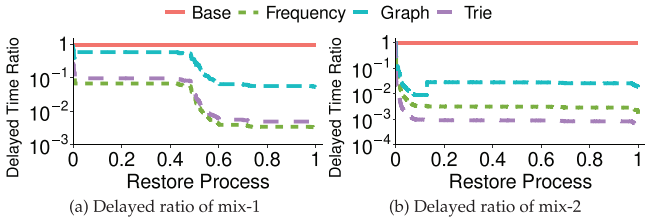

Figure 5: Delayed ratio of two datasets on different restoration approaches. The *x*-axis presents the whole restore process

5.3 Performance Evaluation

In the performance evaluation, we focus on the impact of different storage media, network bandwidth, and the number of users on the three restore approaches compared with the baseline alphabetical approach. Our key findings are as follows:

1) Our three approaches have performed well on different storage media for different datasets. They can reduce the client's delay time by 4×–700× compared to the baseline approach.
2) Increasing the bandwidth of the network can effectively reduce the delay time of users. When the network bandwidth is increased by 10×, the total delayed time of the baseline approach could be reduced by 14.8×, and the other three approaches proposed in this paper can reduce 2.2×~6.2×.
3) Our system's store throughput can reach 829.0 MiB/s, and restore throughput can reach 1083.5 MiB/s with multiple clients.

Exp#1 (Delayed time of restoration approaches). We evaluate the actual cumulated delay time based on two types of storage media during restoration. Here, unlike in the theoretical analysis, we deploy both cloud

and client programs on the host machine to evaluate the cumulated read delay when restoring files from cloud-side HDD to client-side HDD and from cloud-side SSD to client-side SSD.

Figs. 6 and 7 show the results of accumulated delayed time on the client side with the restore process. Obviously, under the condition of SSD storage media, the overall restore time is significantly lower than that of HDD storage media due to higher I/O bandwidth. And under each storage media, the baseline approach (alphabetical order) has the worst performance. In addition, the current access sequence **A** includes access to new files that do not appear in the backup and will not increase the delayed time.

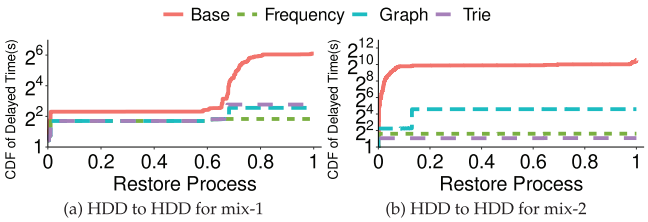

Figure 6: (Exp#1) Cumulative distribution function (CDF) of delayed time of two datasets on different storage media. HDD to HDD means restoring files from the cloud-side HDD to the client-side HDD. The *x*-axis presents the whole restore process

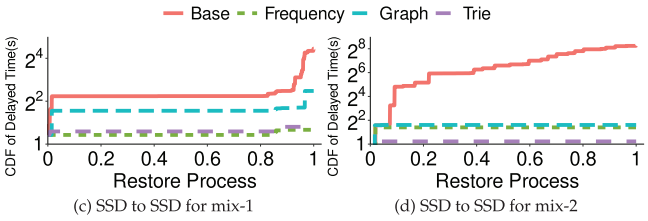

Figure 7: (Exp#1) CDF of delayed time of two datasets on different storage media. SSD to SSD means restoring files from the cloud-side SSD to the client-side SSD. The *x*-axis presents the whole restore process

For the *mix-1* dataset, the frequency-based approach outperforms all approaches with both SSD and HDD storage media. The reason is that the frequency-based approach has a very low computation overhead for generating a restore sequence and has no communication overhead during the restoration process. Under SSD storage media, trie-based and frequency-based approaches have a better performance than HDD. In addition to the reason for the faster read and write speed of SSD, it also shows that trie-based and frequency-based approaches have better performance when the frequently accessed files are small files.

For the *mix-2* dataset, the trie-based approach performs better than the others. The reason it outperforms the other approaches in the *mix-2* dataset but not in the *mix-1* dataset is that the *mix-2*'s access sequence during restoration has higher locality than *mix-1* and the trie-based approach restores files with priority in terms of locality. The graph approach has the longest delay time due to high computation overhead. However, the three approaches have significantly reduced the delay time compared to the baseline approach. Although the graph-based approach has the worst performance, it can still reduce 4× the client's delayed time compared to the baseline approach. While in the best case (*mix-2*), the trie-based approach can reduce up to 700× the client's delayed time compared to the baseline approach.

Exp#2 (Network speed's influence on delay time). To study the impact of network bandwidth on cumulative delayed time, we set up the cloud program on our cloud machine and the client programs on the host machines. In addition, we controlled the network bandwidth at 5, 10, 20, and 50 MiB/s via `trickle` [39].

Fig. 8 shows the results of four approaches to the cumulative delayed time when finishing the restore for the *mix-1* dataset under different network bandwidths. When the network bandwidth is 50 MiB/s, the frequency-based approach could reduce the total delayed time to the lowest 1.08 s. In contrast, when the network bandwidth is reduced to 5 MiB/s, the total delayed time of the frequency-based approach reaches 3.6 s, which is 3.3× that of the former. For comparison, the baseline approach is more seriously affected by the network bandwidth. When the network bandwidth is reduced from 50 to 5 MiB/s, the total delayed time increases by 14.8× to 2357.2 s. Increasing the network bandwidth is effective in reducing the delay time, which mainly comes from two aspects. On the one hand, the cumulative restore time is shortened. On the other hand, increasing the network bandwidth can make the restoration time of all files earlier, so that the files that were not restored at a certain time in the access sequence **A** at a lower network bandwidth may be restored by the high network bandwidth. Overall, the three approaches we introduced have the lower cumulative delay time; the frequency-based approach is the best, followed by the trie-based approach, and the graph-based approach. Note that the graph-based approach incurs the highest delay time over the three approaches due to high computational overhead.

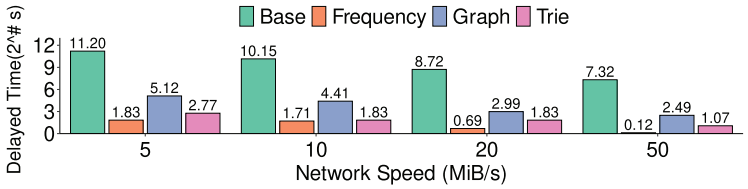

Figure 8: (Exp#2) The cumulative delayed time of the four restore approaches under different network bandwidth (For clarity, the *y*-axis uses a base-2 logarithmic axis)

Exp#3 (Multi-client stores and restores). We evaluate the performance when one or more clients issue Store/Restore concurrently. We extend Exp#2 from two aspects. First, we deploy the clients and the cloud's storage backend in ramdisk. Also, we set each client to store 3.97 GiB files data sampled from *mix-1* dataset to the cloud, and then restore files of the same size from the cloud, and evaluate the *aggregate store (restore) speed* as the ratio of the total stored (restored) data size to the total time all clients finish the stores (restores).

Fig. 9a shows the accumulated store throughput, which is the same for all four approaches due to the files being stored in the order of appearance. The overall store throughput of the system increases with the number of clients first (620.1 MiB/s for one client) and reaches the maximum throughput of 829.0 MiB/s at two clients due to resource contention, then decreases with the increase of the number of clients.

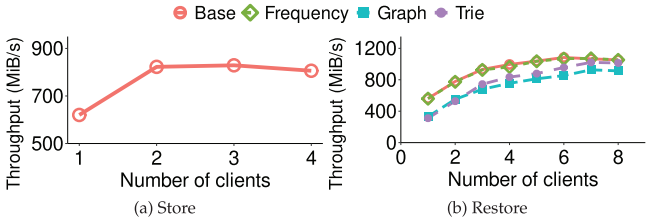

Figure 9: (Exp#3) Multi-client throughput. The store throughput is the same for all four schemes as all files are stored in the order in which they appeared

Fig. 9b shows the accumulated restore throughput vs. the number of clients. The aggregate restores throughput of four approaches increases with the number of clients and finally plateaus when reaching the maximum throughput of 1083.5 MiB/s at 6 clients for the baseline approach and

1072.2, 926.4, and 1021.2 MiB/s at 7 clients for frequency-based, graph-based and trie-based approaches, respectively.

Compared with the baseline approach, the frequency-based approach introduced merely 1.0% performance overhead since it only needs to process the historical sequence once, which has only minimal computing overhead. The graph-based approach has the lowest throughput of the four approaches and introduced 14.5% overhead compared with the baseline approach. The reason is that obtaining the correlation between files for each client requires a fixed computational overhead, which would not change with the number of clients. Since the trie-based approach needs to constantly predict the restore file through the current access file's information, it leads to enormous computational overhead. It has the slowest restore throughput when the client number is small. However, it outperforms the graph-based approach when the number of clients increases since the restore manager uses the file in the default frequency sequence as the target restore file to take the place of the target file that cannot be calculated in time.

6 Related Work

Backup restore. Previous works focus on accelerating restore speed. Cumulus [5] applies segment cleaning to reduce the amount of backup data to be downloaded in the restore procedure. Data deduplication [40,41] introduces *chunk fragmentation* [6] and degrades restore performance. A large body of works [6–8,42] address chunk fragmentation to improve restore speed. This paper focuses on online restoration and preserves the performance of users' foreground operations. In addition, the rapid evolution of blockchain technology [43,44] has significantly advanced data storage infrastructure in recent years. Sokolov et al. [45] proposed improvements to backup restoration leveraging blockchain, while Singh and Batra [46] examined its applications across multiple cloud service providers. Nevertheless, the performance of blockchain-based backup restoration remains constrained by the overhead introduced by consensus mechanisms and communication requirements [47].

Nemoto et al. [48] propose on-demand restore, which recovers directories and files based on users' requests prior to less important ones. This work differs from on-demand restore [48] for automatically scheduling the restore sequence of files.

Table 1 compares Histore with several representative backup restoration approaches. In summary, Histore is the first online backup restoration system to leverage access patterns, achieving superior restoration performance compared to existing approaches.

Table 1: Comparisons between histore and several representative existing backup restoration approaches

Approach	Execution type	Granularity	Key technique	Limitation
[6]	Offline	Block level	Container capping and forward prefetching	Users must wait for the entire backup to restore before accessing data
[48]	Online	File level	On-demand restore	Only a subset of files in the backup is restored
[45]	Online	File level	Blockchain-based strategy for decentralized system	Performance is limited by blockchain's inherent overheads
Ours	Online	File level	Restore sequence scheduling based on access patterns	–

Modeling access patterns. This paper is related to previous works that model historical access patterns from the block level (e.g., [12,49,50]) and the file level [14,15,51–53], in order to predict future access. We focus on modeling the file-level access pattern. The last successor predicts that access to each file will be followed by the same file that followed the last access to the file. Amer and Long [51] extend the last successor model by tracking *access locality* (i.e., some files are more likely to be successively accessed, followed by each file), and makes predictions only for the files with strong access locality. Amer et al. [52] augment Noah with the tunability of the prediction accuracy and the number of predictions made.

In addition to the last successor model, Kroeger et al. [14,53] propose two *context-aware* models to make predictions. The first model builds a graph to track the frequency counts of file accesses within a sliding window, and predicts future access based on the file that is most likely to be accessed after the current file. The second model builds a trie to track file access events via the *multi-order context modeling*, and predicts future access based on the probability that the child's access occurs. EPCM [15] extends the trie-based approach [14,53] to predict the sequence of upcoming file access. Nexus [54] extends the graph-based approach [14] to aggressively prefetch metadata. We highlight that our schemes are focused on generating predicted sequences of restore files rather than individual files.

Additional works (e.g., FARMER [55], SmartStore [56], SANE [57], and SMeta [13]) build *semantic-aware* models on metadata, in order to accelerate metadata queries or improve prefetching accuracy in distributed file systems. However, the semantic-aware models incur high storage overhead for storing the attributes of metadata objects, as well as high computational overhead for counting the similarity degrees of different objects.

7 Conclusion

We present Histore, which exploits correlation among backup files through the user's file historical access information to adapt the backup file restore sequence. Our main concern is to improve the user's access success rate during the restoration period while reducing the user's delayed time under the online restore scenario. We propose three different approaches for generating restore sequences, namely frequency-based, graph-based, and trie-based approaches, and implement a system to evaluate our idea. We discuss the limitations of our current system in terms of scalability and security. We extensively evaluate our system from the theoretical and practical aspects. We show that Histore effectively reduces users' delayed time by 4–700× with only 1.0%–14.5% additional performance overhead while improving the user's file availability during restoration.

Acknowledgement: We would like to express our sincere gratitude to the funding program that supported this work.

Funding Statement: This work was supported in part by National Key R&D Program of China (2022YFB4501200), National Natural Science Foundation of China (62332018), Science and Technology Program (2024NSFTD0031, 2024YFHZ0339 and 2025ZNSFSC0497).

Author Contributions: The authors confirm contribution to the paper as follows: Conceptualization, Ruidong Chen, Guopeng Wang and Ting Chen; methodology, Ruidong Chen, Guopeng Wang, Jingyuan Yang and Xingpeng Tang; software, Jingyuan Yang, Ziyu Wang, Fang Zou and Jia Sun; validation, Ruidong Chen, Guopeng Wang and Ting Chen; resources, Jingyuan Yang, Ziyu Wang, Fang Zou and Jia Sun; data curation, Ziyu Wang, Fang Zou and Jia Sun; writing—original draft preparation, Ruidong Chen, Guopeng Wang, Jingyuan Yang and Ting Chen; writing—review and editing, Jingyuan Yang and Ting Chen; supervision, Ting Chen; funding acquisition, Ting Chen. All authors reviewed the results and approved the final version of the manuscript.

Availability of Data and Materials: Not applicable.

Ethics Approval: Not applicable.

Conflicts of Interest: The authors declare no conflicts of interest to report regarding the present study.

Abbreviations/Acronyms

CDF	Cumulative Distribution Function
LoC	Lines of Code
RAM	Random Access Memory
AMD	Advanced Micro Devices, Inc.
NVMe	Non-Volatile Memory Express
LAN	Local Area Network
HDD	Hard Disk Drive
SSD	Solid State Drive
NVMe	Non-Volatile Memory Express
MSRC	Microsoft Research Cambridge

References

1. Google Cloud [Internet]. [cited 2025 Oct 1]. Available from: https://cloud.google.com/storage.
2. Amazon Cloud Storage. [cited 2025 Oct 1]. Available from: https://aws.amazon.com.
3. Xue K, Chen W, Li W, Hong J, Hong P. Combining data owner-side and cloud-side access control for encrypted cloud storage. IEEE Trans Inf Forensics Secur. 2018;13(8):2062–74. doi:10.1109/TIFS.2018.2809679.
4. Gao Y, Li Q, Tang L, Xi Y, Zhang P, Peng W, et al. When Cloud Storage Meets RDMA. In: 18th USENIX Symposium on Networked Systems Design and Implementation (NSDI 21). Berkeley, CA, USA: USENIX Association; 2021. p. 519–33.
5. Vrable M, Savage S, Voelker GM. Cumulus: filesystem backup to the cloud. ACM Trans Storage. 2009;5(4):1–28. doi:10.1145/1629080.1629084.
6. Lillibridge M, Eshghi K, Bhagwat D. Improving restore speed for backup systems that use inline chunk-based deduplication. In: 11th USENIX Conference on File and Storage Technologies (FAST '13). Berkeley, CA, USA: USENIX Association; 2013. p. 183–97.
7. Fu M, Feng D, Hua Y, He X, Chen Z, Xia W, et al. Accelerating restore and garbage collection in deduplication-based backup systems via exploiting historical information. In: 2014 USENIX Annual Technical Conference. Berkeley, CA, USA: USENIX Association; 2014. p. 181–92.
8. Cao Z, Wen H, Wu F, Du DHC. ALACC: accelerating restore performance of data deduplication systems using adaptive look-ahead window assisted chunk caching. In: 16th USENIX Conference on File and Storage Technologies (FAST 18). Berkeley, CA, USA: USENIX Association; 2018. p. 309–24.
9. Chaudhary J, Vyas V, Saxena M. Backup and restore strategies for medical image database using NoSQL. In: Communication, software and networks. Singapore: Springer Nature; 2022. p. 161–71. doi:10.1007/978-981-19-4990-6_15.
10. Bogatyrev VA, Bogatyrev SV, Bogatyrev AV. Recovery of real-time clusters with the division of computing resources into the execution of functional queries and the restoration of data generated since the last backup. In: Distributed computer and communication networks: control, computation, communications. Cham, Switzerland: Springer Nature; 2024. p. 236–50. doi:10.1007/978-3-031-50482-2_19.
11. Tang X, Li J. Improving online restore performance of backup storage *via* historical file access pattern. In: Frontiers in cyber security. Singapore: Springer Nature; 2022. p. 365–76. doi:10.1007/978-981-19-8445-7_23.
12. Liao J, Trahay F, Gerofi B, Ishikawa Y. Prefetching on storage servers through mining access patterns on blocks. IEEE Trans Parallel Distrib Syst. 2016;27(9):2698–710. doi:10.1109/TPDS.2015.2496595.
13. Chen Y, Li C, Lv M, Shao X, Li Y, Xu Y. Explicit data correlations-directed metadata prefetching method in distributed file systems. IEEE Trans Parallel Distrib Syst. 2019;30(12):2692–705. doi:10.1109/TPDS.2019.2921760.

14. Kroeger TM, Long DDE. The case for efficient file access pattern modeling. In: Proceedings of the Seventh Workshop on Hot Topics in Operating Systems; 1999 Mar 30–30; Rio Rico, AZ, USA. Piscataway, NJ, USA: IEEE; 2002. p. 14–9. doi:10.1109/HOTOS.1999.798371.
15. Kroeger TM, Long DD. Design and implementation of a predictive file prefetching algorithm. In: 2001 USENIX Annual Technical Conference (USENIX ATC 01); 2001 Jun 25–30; Boston, MA, USA; 2001. p. 105–18.
16. Li J, Nelson J, Michael E, Jin X, Ports DR. Pegasus: tolerating skewed workloads in distributed storage with in-network coherence directories. In: 14th USENIX Symposium on Operating Systems Design and Implementation (OSDI 20). Berkeley, CA, USA: USENIX Association; 2020. p. 387–406.
17. Zou X, Xia W, Shilane P, Zhang H, Wang X. Building a high-performance fine-grained deduplication framework for backup storage with high deduplication ratio. In: Proceeding of 2022 USENIX Annual Technical Conference. Berkeley, CA, USA: USENIX Association; 2022. p. 19–36.
18. Yang J, Wu J, Wu R, Li J, Lee PP, Li X, et al. ShieldReduce: fine-grained shielded data reduction. In: USENIX ATC '25: Proceedings of the 2025 USENIX Conference on Usenix Annual Technical Conference; 2025 Jul 7–9; Boston, MA, USA. p. 1281 –96.
19. Restore your iPhone, iPad, or iPod Touch from a Backup [Internet]. 2020 [cited 2025 Oct 1]. Available from: https://support.apple.com/en-us/HT204184.
20. Douceur JR, Bolosky WJ. A large-scale study of file-system contents. SIGMETRICS Perform Eval Rev. 1999;27(1):59–70. doi:10.1145/301464.301480.
21. Tang Y, Li D, Li Z, Zhang M, Jee K, Xiao X, et al. NodeMerge: template based efficient data reduction for big-data causality analysis. In: Proceedings of the 2018 ACM SIGSAC Conference on Computer and Communications Security. New York, NY, USA: The Association for Computing Machinery (ACM); 2018. p. 1324–37. doi:10.1145/3243734.3243763.
22. Cheng X, Dale C, Liu J. Statistics and social network of YouTube videos. In: 2008 16th Interntional Workshop on Quality of Service; 2008 Jun 2–4; Enschede, The Netherlands; 2008. p. 229–38. doi:10.1109/IWQOS.2008.32.
23. Lyu F, Ren J, Cheng N, Yang P, Li M, Zhang Y, et al. LeaD: large-scale edge cache deployment based on spatio-temporal WiFi traffic statistics. IEEE Trans Mob Comput. 2021;20(8):2607–23. doi:10.1109/TMC.2020.2984261.
24. Shvachko K, Kuang H, Radia S, Chansler R. The hadoop distributed file system. In: 2010 IEEE 26th Symposium on Mass Storage Systems and Technologies (MSST); 2010 May 3–7; Incline Village, NV, USA. Piscataway, NJ, USA: IEEE; 2010. p. 1–10. doi:10.1109/msst.2010.5496972.
25. Ousterhout JK, Da Costa H, Harrison D, Kunze JA, Kupfer M, Thompson JG. A trace-driven analysis of the UNIX 4.2 BSD file system. In: Proceedings of the Tenth ACM Symposium on Operating Systems Principles. New York, NY, USA: The Association for Computing Machinery (ACM); 1985. p. 15–24. doi:10.1145/323647.323631.
26. LevelDB [Internet]. 2011 [cited 2025 Oct 1]. Available from: https://github.com/google/leveldb.
27. Binary search tree [Internet]. 1960 [cited 2025 Oct 1]. Available from: https://en.wikipedia.org/wiki/Binary_search_tree.
28. Luo R, He Q, Xu M, Chen F, Wu S, Yang J, et al. Edge data deduplication under uncertainties: a robust optimization approach. IEEE Trans Parallel Distrib Syst. 2025;36(1):84–95. doi:10.1109/TPDS.2024.3493959.
29. Ren Y, Ren Y, Li X, Hu Y, Li J, Lee PP. ELECT: enabling erasure coding tiering for LSM-tree-based storage. In: 22nd USENIX Conference on File and Storage Technologies (FAST 24); 2024 Feb 26–29; Santa Clara, CA, USA. p. 293–310.
30. Li J, Yang Z, Ren Y, Lee PPC, Zhang X. Balancing storage efficiency and data confidentiality with tunable encrypted deduplication. In: Proceedings of the Fifteenth European Conference on Computer Systems. New York, NY, USA: The Association for Computing Machinery (ACM); 2020. p. 1–15. doi:10.1145/3342195.3387531.
31. Yang W, Gong X, Chen Y, Wang Q, Dong J. SwiftTheft: a time-efficient model extraction attack framework against cloud-based deep neural networks. Chin J Electron. 2024;33(1):90–100. doi:10.23919/cje.2022.00.377.
32. Li J, Ren Y, Lee PPC, Wang Y, Chen T, Zhang X. FeatureSpy: detecting learning-content attacks via feature inspection in secure deduplicated storage. In: IEEE INFOCOM, 2023-IEEE Conference on Computer Communications; 2023 May 17–20; New York City, NY, USA. Piscataway, NJ, USA: IEEE; 2023. p. 1–10. doi:10.1109/INFOCOM53939.2023.10228971.

33. Stefanov E, Dijk MV, Shi E, Chan TH, Fletcher C, Ren L, et al. Path ORAM: an extremely simple oblivious RAM protocol. J ACM. 2018;65(4):1–26. doi:10.1145/3177872.
34. Li X, Luo Y, Gao M. Bulkor: enabling bulk loading for path ORAM. In: 2024 IEEE Symposium on Security and Privacy (SP); 2024 May 19–23; San Francisco, CA, USA. Piscataway, NJ, USA: IEEE; 2024. p. 4258–76. doi:10.1109/sp54263.2024.00103.
35. Process Monitor [Internet]. [cited 2025 Oct 1]. Available from: https://docs.microsoft.com/en-us/sysinternals/downloads/procmon.
36. FSL Traces and Snapshots Public Archive [Internet]. 2014 [cited 2025 Oct 1]. Available from: http://tracer.filesystems.org/.
37. SNIA. Microsoft research cambridge target block traces. [cited 2025 Oct 1]. Available from: http://iotta.snia.org/traces/block-io/388.
38. Microsoft UBC-Dedup Traces [Internet]. [cited 2025 Oct 1]. Available from: http://iotta.snia.org/traces/static/3382.
39. Eriksen MA. Trickle: a userland bandwidth shaper for UNIX-like systems. In: FREENIX Track: 2005 USENIX Annual Technical Conference. Berkeley, CA, USA: USENIX Association; 2005. p. 61–70.
40. Yang Z, Li J, Lee PP. Secure and lightweight deduplicated storage via shielded deduplication-before-encryption. In: 2022 USENIX Annual Technical Conference (USENIX ATC 22). Berkeley, CA, USA: USENIX Association; 2022. p. 37–52.
41. Zhao J, Yang Z, Li J, Lee PPC. Encrypted data reduction: removing redundancy from encrypted data in outsourced storage. ACM Trans Storage. 2024;20(4):1–30. doi:10.1145/3685278.
42. Cao Z, Liu S, Wu F, Wang G, Li B, Du DH. Sliding look-back window assisted data chunk rewriting for improving deduplication restore performance. In: 17th USENIX Conference on File and Storage Technologies. Berkeley, CA, USA: USENIX Association; 2019. p. 129–42.
43. Yang K. Zero-cerd: a self-blindable anonymous authentication system based on blockchain. Chin J Electron. 2023;32(3):587–96. doi:10.23919/cje.2022.00.047.
44. Su J. A hybrid entropy and blockchain approach for network security defense in SDN-based IIoT. Chin J Electron. 2023;32(3):531–41. doi:10.23919/cje.2022.00.103.
45. Sokolov S, Vlaev S, Iliev TB. Technique for improvement of backup and restore strategy based on blockchain. In: 2022 International Conference on Communications, Information, Electronic and Energy Systems (CIEES); 2022 Nov 24–26; Veliko Tarnovo, Bulgaria. p. 1–6. doi:10.1109/CIEES55704.2022.9990781.
46. Amanpreet S, Jyoti B. Strategies for data backup and recovery in the cloud. Int J Perform Eng. 2023;19(11):728. doi:10.23940/ijpe.23.11.p3.728735.
47. Shi D. RESS: a reliable and effcient storage scheme for Bitcoin blockchain based on Raptor code. Chin J Electron. 2023;32(3):577–86. doi:10.23919/cje.2022.00.343.
48. Nemoto J, Sutoh A, Iwasaki M. File system backup to object storage for on-demand restore. In: 2016 5th IIAI International Congress on Advanced Applied Informatics (IIAI-AAI); 2016 Jul 10–14; Kumamoto, Japan. p. 946–52. doi:10.1109/iiai-aai.2016.116.
49. Li Z, Chen Z, Srinivasan SM, Zhou Y, et al. C-Miner: mining block correlations in storage systems. In: 3rd USENIX Conference on File and Storage Technologies (FAST 04). Berkeley, CA, USA: USENIX Association; 2004.
50. Soundararajan G, Mihailescu M, Amza C. Context-aware prefetching at the storage server. In: ATC'08: USENIX, 2008 Annual Technical Conference; 2008 Jun 22–27; Boston, MA, USA. p. 377 –90.
51. Amer A, Long DD. Noah: low-cost file access prediction through pairs. In: Proceedings of the 2001 IEEE International Performance, Computing, and Communications Conference; 2001 Apr 4–6; Phoenix, AZ, USA. p. 27–33.
52. Amer A, Long DDE, Paris JF, Burns RC. File access prediction with adjustable accuracy. In: Proceedings of the IEEE International Performance, Computing, and Communications Conference; 2002 Apr 3–5; Phoenix, AZ, USA. p. 131–40.
53. Kroeger TM, Long DDE. Predicting file system actions from prior events. In: USENIX 1996 Annual Technical Conference (USENIX ATC 96). Berkeley, CA, USA: USENIX Association; 1996.

54. Gu P, Zhu Y, Jiang H, Wang J. Nexus: a novel weighted-graph-based prefetching algorithm for metadata servers in petabyte-scale storage systems. In: Sixth IEEE International Symposium on Cluster Computing and the Grid (CCGRID'06); 2006 May 16–19; Singapore. doi:10.1109/CCGRID.2006.73.
55. Xia P, Feng D, Jiang H, Tian L, Wang F. FARMER: a novel approach to file access correlation mining and evaluation reference model for optimizing peta-scale file system performance. In: Proceedings of the 17th International Symposium on High Performance Distributed Computing. New York, NY, USA: The Association for Computing Machinery (ACM); 2008. p. 185–96. doi:10.1145/1383422.1383445.
56. Hua Y, Jiang H, Zhu Y, Feng D, Tian L. SmartStore: a new metadata organization paradigm with semantic-awareness for next-generation file systems. In: Proceedings of the Conference on High Performance Computing Networking, Storage and Analysis; 2009 Nov 14–20; Portland, OR, USA. p. 1–12.
57. Hua Y, Jiang H, Zhu Y, Feng D, Xu L. SANE: semantic-aware namespacein ultra-large-scale file systems. IEEE Trans Parallel Distrib Syst. 2014;25(5):1328–38. doi:10.1109/TPDS.2013.140.